Inversion Preprocessing Transfer Function for the Helmholtz Equation

Matthew Yedlin[a], Daryl Van Vorst[a], Jean Virieux[b]

[a]*Department of Electrical and Computer Engineering, University of British Columbia, 2332 Main Mall, UBC Campus, Vancouver, Canada*
[b]*Laboratoire de Gophysique Interne et Tectonophysique - LGIT, BP 53, 38041 Grenoble CEDEX 9 France*

Abstract

The conversion of a three-dimensional acoustic data set into an equivalent two-dimensional acoustic data set are essential for seismic interpretation where the amplitude is a key issue. The transfer function for such a transformation should be estimated and we propose to proceed to this construction through the computation of the pressure field when considering the Helmholtz equation. Ray theory is used in order to improve the homogeneous transfer function that is typically applied to three-dimensional data to obtain the input two-dimensional data set used in many inversion algorithms. The improved transfer function uses a uniform expansion that directly includes the source singularity. The entire useful frequency bandwidth is more accurately preserved by using the uniform expansion. A synthetic example is presented for the Helmholtz equation for the borehole geometry encountered in cross-well radar experiments.

Keywords: Transfer function, Helmholtz equation, uniform asymptotic expansion, ray tracing

1. Introduction

Considerable effort and expertise has been expended in inverting acquired three-dimensional data in applied geophysics, significantly in whole earth seismology, exploration seismology and in near-surface geophysical applications. Moreover, recent investigations such as full waveform inversion exploits preserved or true amplitudes of seismic signals in a broad frequency range. In this paper we will present a pre-processing step which will transform data collected in the real three dimensional Earth into data as if it were collected in a two dimensional domain. The methodology is presented in the context of the Helmholtz equation, but it can be extended to more general wave equations, appearing in ground-penetrating radar (GPR) or in elastodynamics. In the context of inversion, preserving the entire bandwidth in current broadband recording (Pratt et al., 1996, 1998) is a critical feature in any data transformation such as the transfer function obtained through uniform asymptotic expansions of the solution of the Helmholtz equation in two and three dimensions.

2. Theory

2.1. Ray Tracing Background

In this section, we will briefly review the common ray tracing ansatz and describe where it breaks down when considering the solution near the source. References are available in the review article (Virieux and Lambaré,

*Corresponding Author: Matthew Yedlin, Department of Electrical and Computer Engineering, University of British Columbia, 2332 Main Mall, Vancouver, B.C., Canada. Tel.: 1 604 822 8236; fax: 1 604 822 5949

Email address: matty@ece.ubc.ca (Matthew Yedlin)

2007). The equation which we will use throughout this article is the two or three-dimensional Helmholtz equation for the pressure field. In three dimensions, this equation is given by

$$\nabla^2 P + \frac{\omega^2}{v^2(x,y,z)} P = \delta(x-x')\delta(y-y')\delta(z-z'), \tag{1}$$

where the pressure field is denoted by P, the angular frequency by ω and the wave velocity by $v(x,y,z)$. The Cartesian coordinate system has been implicitly introduced. An analogous equation holds in two dimensions and is given by

$$\nabla^2 P + \frac{\omega^2}{v^2(x,z)} P = \delta(x-x')\delta(z-z'). \tag{2}$$

The standard ansatz used for the ray tracing solution (Karal and Keller, 1959; Keller, 1978) in a three-dimensional medium is given by

$$P(x,y,z,\omega) = exp(-i\omega T(x,y,z)) \sum_{n=0}^{\infty} \frac{A_n(x,y,z)}{(i\omega)^n}, \tag{3}$$

where $T(x,y,z)$ is the travel-time function and the terms A_n are a set of amplitude coefficients. The usual technique is to substitute the ansatz (3) into the inhomogeneous Helmholtz equation (1) in order to obtain a hierarchy of equations by setting each coefficent of powers of ω to zero. The coefficient of ω^2 is the eikonal equation given by

$$[\nabla T(x,y,z)]^2 = \frac{1}{v^2(x,y,z)}. \tag{4}$$

Please note the natural introduction of the square of the slowness, the inverse of the velocity.

The remaining equations in the hierarchy are the transport equations for the coefficients in the ansatz (3) and are given by

$$\left[2\left(\nabla A_n \cdot \nabla T\right) + A_n \nabla^2 T\right] = -\nabla^2 A_{n-1}, n = 0, 1, \cdots, \tag{5}$$

where we have dropped out the arguments of these terms. Once the travel-time function $T(x, y, z)$ has been computed, in principal, the solutions to the transport equation hierarchy can be obtained recursively. In general at most two coefficients in the hierarchy are computed for computing the pressure solution, with the challenge being the calculation of the Laplacian of the travel-time function. While it is well-known that $T(x, y, z)$ can be multi-valued, we consider the case in which the travel-time is single-valued in this paper.

One could compute the travel-time function, $T(x, y, z)$, through wavefront evolution by solving the eikonal equation (4) (Vidale, 1988, 1990; Lambaré et al., 1996; Zhao, 2005) or through the method of characteristics (Courant and Hilbert, 1966). For the second method, a set of coupled ordinary differential equations need to be solved. The first set, describes the tangent unit vector $\hat{t}$ to the ray, which in isotropic media is normal to the level surfaces of $T(x, y, z)$ which represent the wavefront. Therefore, if we paramaterize progression along the ray by the arclength s, directly from the eikonal equation, we obtain the unit tangent vector given by

$$\begin{aligned} \hat{t} &= v\nabla T \\ &= \left(\frac{dx}{ds}, \frac{dy}{ds}, \frac{dz}{ds}\right). \end{aligned} \tag{6}$$

The second set of differential equations describes the curvature, or rate of change of the unit tangent vector, and is given by

$$\frac{d\hat{t}}{ds} = -\frac{1}{v}\nabla \ln v. \tag{7}$$

There is a well-known issue with the solution to the transport equations that is embedded in the calculation of the Laplacian of the travel-time function,

$T(x, y, z)$. There can be singular curves, known as line caustics, or focal points, known as point caustics, at which $\nabla^2 T(x, y, z)$ is undefined. The problem with these singular curves is obviated by using the KMAH index for matching solutions before and after these caustics with an increment of a 90° phase shift for line caustics and a 180° phase shift for point caustics. However, the proper representation of an initial focal point, the source function for the Helmholtz equation, is not as easy as we do not have the solution before crossing this focal point. We discuss this important issue in the next section by considering an ad-hoc asymptotic expansion.

2.2. Uniform Asymptotic Ray Expansions

In the classical calculation of the amplitude coefficients, the cross-sectional area of a ray tube is computed via an appropriate Jacobian, and the ratio of the square roots of Jacobians is used to obtain a new amplitude value from a previous amplitude value (Cerveny, 2001). Since the Jacobian vanishes at a point source in three dimensions or a line source in two dimensions, the foregoing ray method is not sufficient and we must proceed differently. That involves surrounding either the point source or line source by a homogeneous medium on the boundaries of which both travel-times and initial ray amplitude can be computed. Since we know the exact Green's function for the case of a homogeneous medium in either three or two dimensions, we must estimate the initial values of the ray amplitudes on the boundary separating the homogeneous region from the surrounding inhomogeneous region. A problem with this solution, is that it is not clear where the homogeneous region should end and where the true inhomogeneous region should begin. Such a matching technique, based on canonical problems, is termed

non-uniform.

To alleviate this problem, we modify the ansatz used in the ray method. The solution is singular at the source which is a line caustic in two dimensions and a point caustic in three dimensions (Zauderer, 1970). In the conventional ansatz, (3), we are trying to model the singularity of the source by a "smooth" expansion. Therefore, reshaping the ray ansatz could be achieved through the replacement of the plane wave eikonal formulation consisting only of the phase term by an alternative ansatz which includes an appropriate amplitude correction. The motivation for choosing this ansatz derives from the exact three-dimensional and two-dimensional solutions as represented by the Green's function for the Helmholtz equation in a homogeneous acoustic medium. Thus we automatically include the source singularity.

2.2.1. Three-Dimensional Uniform Ansatz

For the three dimensional case, the uniform expansion is given by (Yedlin and Virieux, 2010)

$$P(x,y,z) = -\frac{exp(-i\omega T(x,y,z))}{4\pi v(x,y,z)T(x,y,z)} \sum_{n=0}^{\infty} \frac{A_n(x,y,z)}{(i\omega)^n}. \tag{8}$$

The travel-time function $T(x,y,z)$ represents the wavefront travel-time and the set of $A_n(x,y,z)$ comprises the asymptotic expansion coefficients, which represent the amplitudes. In contrast to the two-dimensional problem to be discussed below, the three-dimensional problem only requires one expansion (Avila and Keller, 1963). A different formulation of the uniform expansion is also given by Babich (Babich, 1965, 1991).

Substitution of the expression (8) into the Helmholtz equation (1) results in the usual hierarchy of equations by setting coefficients of powers of ω to

zero. As for the standard ansatz, the leading term in the hierarchy gives the eikonal equation (4). A modified transport equation is obtained, which can be solved recursively. In this research, we will focus only on the first term of the expansion, which dominates for high frequencies. The transport equations for $A_0(x, y, z)$ in three dimensions is given by

$$2\nabla T(x, y, z) \cdot \nabla B_0(x, y, z) + B_0(x, y, z)\nabla^2 T(x, y, z) = 0, \tag{9}$$

with

$$B_0(x, y, z) = \frac{A_0(x, y, z)}{v(x, y, z)T(x, y, z)}. \tag{10}$$

Dropping the explicit dependence on the coordinates (x, y, z) and using the directional derivative along a ray parameterized by the arc-length s, we obtain the operator equivalence defined by

$$2\nabla T \cdot \nabla = \frac{2}{v}\frac{d}{ds}. \tag{11}$$

Using (11), we can re-write the transport equation (9) as an ordinary differential equation along the ray as a function of the arc length s. The initial conditions, in three dimensions, depend on two parameters describing the behaviour off the ray, q_1 and q_2. Therefore, as shown by Cerveny (2001), we have

$$\frac{2}{v}\frac{d}{ds}\left(\frac{A_0}{vT}\right) + \frac{A_0}{vT}\frac{1}{J}\frac{d}{ds}\left(\frac{J}{v}\right) = 0, \tag{12}$$

where the Jacobian of the ray transformation J is directly related to an element of wavefront dS around the ray under consideration. That is,

$$dS = Jd\Omega = Jdq_1dq_2. \tag{13}$$

We may insist that the Jacobian estimation depends on the coordinate system that we are free to select. Completeness is provided by the summation

over a sphere of arbitrarily small radius R, such that

$$4\pi R^2 = S = \int_R dS = \int_R J d\Omega = J \int_R d\Omega = 4\pi J, \tag{14}$$

where the Jacobian $J = J_\Omega$ is per solid angle. If one wants to consider specific coordinates as take-off angles, which are usual parameters for the off-ray spatial evolution related to a specific Jacobian J_q, we have the explicit relation $J_q = J_\Omega \sin\theta_0$ as the surface coordinate element is $d\Omega_0 = \sin\theta_0 d\theta_0 d\phi_0$ where the initial dipping angle is θ_0 and the initial azimutal angle is ϕ_0. The solution of the transport equation (12) is given as a function of the arc length s by

$$A_0(s) = \sqrt{\frac{v(s)^3 T^2(s)/J_\Omega(s)}{v(s_0)^3 T(s_0)^2/J_\Omega(s_0)}}\ A(s_0). \tag{15}$$

In the limit as the source arc length s_0 approaches the true source location 0, the amplitude $A(s_0)$ approaches the unity. Both $v(s_0)^2 T(s_0)^2$ and $J_\Omega(s_0)$ approach R^2. Combining these results and letting the quantity s_0 approach zero yields

$$A_0(s) = \sqrt{\frac{v(s)^2 T(s)^2}{J_\Omega(s)}} \sqrt{\frac{v(s)}{v(s_0)}}. \tag{16}$$

Substitution of the amplitude expression (16) into the ansatz (8), while keeping only the first term in the sum, results in the final representation of our pressure field, given by

$$\begin{aligned} P(s) &= -\frac{1}{4\pi} \frac{A_0(s)}{v(s)T(s)} e^{-i\omega T(s)} \\ &= -\frac{1}{4\pi} \frac{1}{\sqrt{J_\Omega(s)}} \sqrt{\frac{v(s)}{v(s_0)}}\ e^{-i\omega T(s)}. \end{aligned} \tag{17}$$

In the equation (17), the ray is parameterized by the arc length s which implicitly is a function of all three spatial coordinates. Besides the arc

length, the ray is also parameterized by two additional parameters, which are related to the Jacobian calculation. We shall use the two angles θ and ϕ sampling the domain off of the ray in our specific applications. The equation (17) is one ingredient of the contruction of our transfer function, while we need to derive the second ingredient through the uniform ansatz in two dimensions.

2.2.2. Two-Dimensional Uniform Ansatz

Due to the nature of wave propagation in two dimensions, designing a uniform expansion that includes the source singularity is much more complicated. Thus, the Green's function does not have a simple oscillating structure as in three-dimensional geometry. The Hankel function H_0^2, which is the two-dimensional Green's function, when expanded in the far field via the appropriate asymptotic expansion, has an exponential phase term. Following the ansatz proposition of Yedlin (1987), we mau consider the following two-dimensional ansatz:

$$\begin{aligned} P(x,z) = & - \frac{1}{4i} H_0^{(2)}\left(\omega T(x,z)\right) \sum_{n=0}^{\infty} \frac{A_n(x,z)}{(i\omega)^n} \\ & - \frac{1}{i\omega}\left[\omega T(x,z)\right] H_1^{(2)}\left(\omega T(x,z)\right) \sum_{n=0}^{\infty} \frac{B_n(x,z)}{(i\omega)^n}. \end{aligned} \tag{18}$$

The reason for considering two terms can be understood through the behaviour of the two-dimensional wave equation. Far away from the source, it is exponential in nature, while near the source, the quasi-static version of the equation is logarithmic, a direct consequence of the fact that we are solving a Poisson equation. This contrasts strongly with the three-dimensional wave equation, which uniformly approaches the inverse distance singularity, as the distance from the source tends to zero.

Substitution of this ansatz (18) into the Helmholtz equation (2) results again in the eikonal equation in two dimensions and a coupled set of transport equations. We will need to compute $T(x,z)$ via the eikonal equation and the amplitude $A_0(x,z)$ via a modified transport equation. The transport equation this time is much simpler than the the 3D equation (9) and is given by

$$2\nabla T(x,z)\cdot\nabla A_0(x,z)+\left[\nabla^2 T(x,z)-\frac{(\nabla T(x,z))^2}{T(x,z)}\right]A_0(x,z)=0. \quad (19)$$

Following the same procedure as in the thre-dimensional case, we convert the transport equation (19) into an ordinary differential equation for $A_0(s)$:

$$\frac{1}{A_0(s)}\frac{d\ A_0(s)}{ds}+\frac{1}{2}\left[\frac{v(s)}{J(s)}\frac{d}{ds}\left(\frac{J(s)}{v(s)}\right)-\frac{1}{T(s)}\frac{dT(s)}{ds}\right]=0, \quad (20)$$

where the Jacobian is such that $2\pi R=\int_R Jd\theta=2\pi J$ for a circle of arbitrarily small radius R. The solution can be written as the expression

$$A_0(s)=\sqrt{\frac{v(s)T(s)/J(s)}{v(s_0)T(s_0)/J(s_0)}}\ A(s_0). \quad (21)$$

Since the wavefront radius of curvature is equal to the product of the velocity and the wavefront travel-time, in the limit as the source arc length s_0 approaches the source value 0, the amplitude term $A(s_0)$ approaches unity and so does the ratio $v(s_0)T(s_0)/J(s_0)$. Therefore, one may express the leading amplitude term as

$$A_0(s)=\sqrt{\frac{v(s)T(s)}{J(s)}}. \quad (22)$$

Substitution of the amplitude expression (22) into the leading term of the 2D ansatz (18) results in our final asymptotic solution for the two-dimensional

pressure field, given by

$$P(s) = -\frac{1}{4i} H_0^2(\omega T(s)) \sqrt{\frac{v(s)T(s)}{J(s)}}. \tag{23}$$

We will now use this two-dimensional pressure field and the three-dimensional pressure field given by (17) for the construction of the desired transfer function.

2.3. Transfer Function Algorithm

The purpose of the transfer function to convert the three-dimensional data collected in the field into two-dimensional data which will be used for inversion. In order to do this, we equate the ratio of data to the pressure fields obtained previously. Thus we have

$$\frac{3DData}{3DPressurefield} = \frac{2DData}{2DPressurefield}. \tag{24}$$

The previous ratio can be viewed as equating the two data fields after the division as a deconvolution. Thus we can define our transfer function denoted by TF as the ratio of the 2D solution (23) to the 3D solution (17), which leads us to the asymptotic expression

$$TF = \left[-\frac{1}{4i} H_0^2(\omega T(s)) \sqrt{\frac{v(s)T(s)}{J_{2D}(s)}} \right] / \left[-\frac{1}{4\pi} \sqrt{\frac{1}{J_{3D}(s)}} \sqrt{\frac{v(s)}{v(0)}} e^{-i\omega T(s)} \right], \tag{25}$$

where the pure imaginary complex number is denoted by i. In the far field, we can expand the Hankel function asymptotically through the equation

$$H_0^2(\omega T(s)) \sim \sqrt{\frac{2}{\pi \omega T(s)}} e^{-i\omega T(s)} e^{i\pi/4} \tag{26}$$

and we obtain the approximate far-field asymptotic transfer function as

$$TF = \sqrt{\frac{2\pi v(0)}{\omega}} \sqrt{\frac{J_{3D}(s)}{J_{2D}(s)}}\, exp\left(-i\frac{\pi}{4}\right). \tag{27}$$

The far-field asymptotic transfer function defined by the expression (27) is the operator to be used in inhomogeneous acoustic media, for which ray theory is valid, and is an extension of the results presented by Bleistein (Bleistein, 1986) and Williamson (Williamson and Pratt, 1995). If we are not in the far field, then the full asymptotic expression (25) should be used. The expression (27) includes source effects in a uniform fashion: it is a generalization of the results presented by Ernst et al. (2007) based on the work of Bleistein (Bleistein, 1986).

3. Numerical Experiments

In this section, we present a numerical illustration of the transfer function application which has been derived in the previous section. To illustrate the method, we choose a vertically inhomogeneous medium with $v(z) = 1/\sqrt{a+bz}\ m/s$, where $a = 1\ \mathrm{s}^2/\mathrm{m}^2$ and $b = -0.08\ \mathrm{s}^2/\mathrm{m}^3$ which is related to the square of the slowness providing the simple analytical solution one can think about when considering non-homogeneous media. The two-dimensional domain is chosen to be a region of 10 m by 10 m, while the three-dimensional domain has the same two-dimension extension with an additional transverse dimension of 5 m. Both solutions are computed using a finite difference Helmholtz solver with $\Delta x = \Delta y = \Delta z = 1/30$ of the shortest wavelength. The computational domain is surrounded by a stretched coordinate perfectly matched layer (Chew et al., 1997). The frequency is 1 Hz, with the point source located at $(x = 0,\ y = 0,\ z = 0)$

in three dimensions, and a line source at $(x = 0, z = 0)$ in two dimensions. In Fig. 1, results from the two-dimensional finite-difference Helmholtz solver are presented. In Fig. 2, a slice of the three-dimensional data volume, corresponding to $(x,\ y = 0,\ z)$ is shown. Comparison of these figures clearly shows the difference in amplitudes of the two and three-dimensional wavefields.

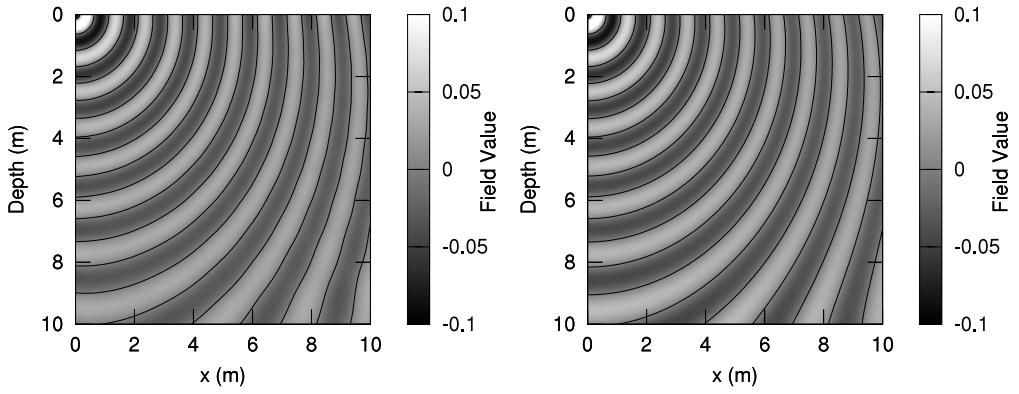

(a) (b)

Figure 1: Real part of the wave-field obtained (a) using the two-dimensional finite difference solver for the Helmholtz equation, and (b) using numerical or analytical ray tracing.

In order to implement the transfer function (27), the wavefield travel-time function $T(x, z)$ is needed as well as the Jacobian. We have computed the travel-time field and consequently associated rays using two methods: a fast sweeping method for the eikonal equation (Zhao, 2005) described as numerical wavefront ray tracing (opposedto the numerical standard ray tracing (Courant and Hilbert, 1966)) and the analytical solution for the square of the slowness (Cerveny, 2001), which are indistinguishable as shown in Fig. 3:

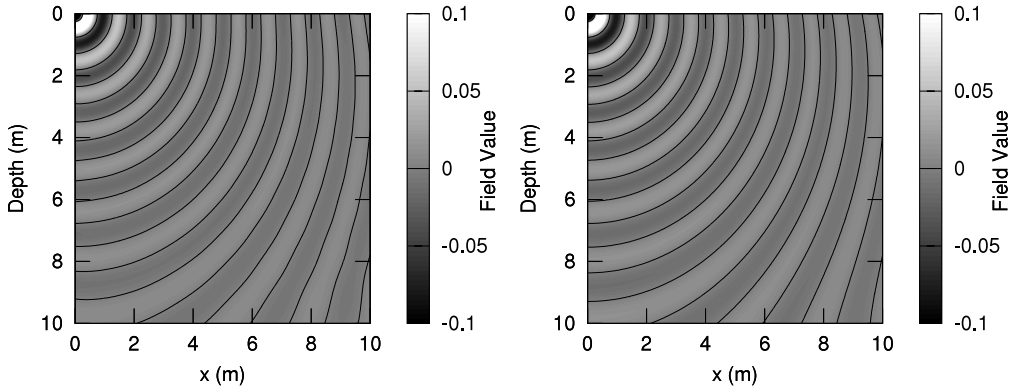

(a) (b)

Figure 2: Real part of the wavefield obtained (a) using the three-dimensional finite difference solver for the Helmholtz equation, and (b) using numerical or analytical ray tracing.

rays end at a set of vertical borehole receivers located at $x = 10\ m$. In the wavefront ray tracing strategy, rays are obtained by following the travel-time gradient backwards from each receiver to the source along with travel-time contours at one second intervals and match exactly the analytical solution as we have verified. Once the ray is given, computing numerically the Jacobian is performed by solving the paraxial ray tracing which matches exactly the analytical solution given by Virieux (1996). We, therefore, have ingredients for computing the transfer function in this inhomogeneous simple medium, but we could consider for realistic applications more complex media through the numerical ray tracing we have implemented. Fig. 4 is a comparison of numerical transfer function by taking the ratio of the 2D and 3D finite-difference solutions of the Helmholtz equation and of those asymptotic transfer function using the complete expression (25) and the far-

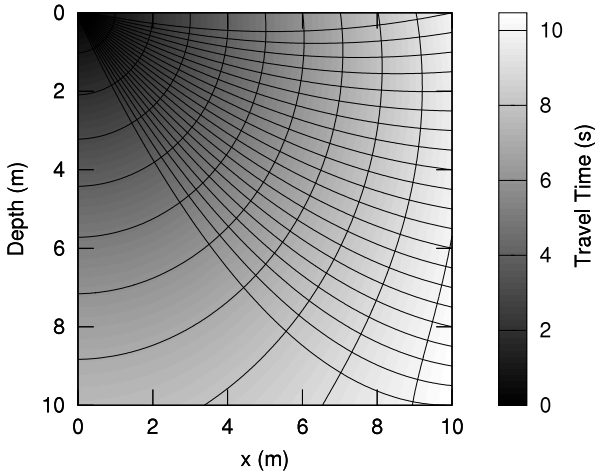

Figure 3: Travel-time field computed using the fast sweeping method, with the associated rays and travel-time contours.

field approximation (27). The phase and modulus of the transfer function are shown separately for all borehole locations at $x = 10\ m$ and z ranging from 0 m to 10 m. The numerical transfer function phase oscillates within 1° of the far-field asymptotic result of -45°. Similarly, the modulus of the numerical transfer function is extremely close to the modulus obtained for both the asymptotic transfer function and its far-field approximation. The foregoing validates the proposed candidate, the expression (25) and the approximation (27) for the transfer function.

We apply these two transfer functions to the three-dimensional wavefield computed numerically (see Fig.2a), obtaining simulated 2D wavefields (see Fig. (5)) which are close to the numerically computed wavefield (see Fig.1a), illustrating the accurate transformation obtained by the asymptotic transfer functions. Fig. 6 represents the relative error which shows that we dramatically improve the precision of the transfer function trans-

formation by using the full asymptotic transfer function we have designed and not its far-field approximation, underlining the accuracy of ansatzs we have proposed for 3D and 2D asymptotic solutions near the source.

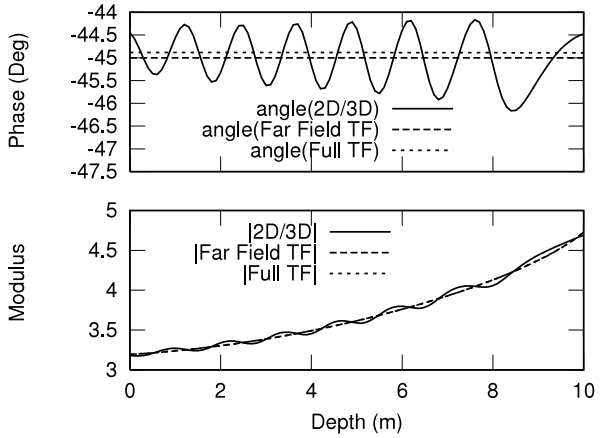

Figure 4: Comparison of phase (upper panel) and modulus (lower panel) of numerical, full and far-field asymptotic transfer functions with gradient $b = -0.08\ s^2/m^3$.

4. Discussion

Although the asymptotic transfer function we have built is quite accurate, some departures from exact ratio between numerical 2D and 3D solutions are observed. These deviations are coming from the ray approximation as we are confident in numerical solutions of the Helmholtz equation with minimal numerical dispersion since we have considered a minimal wavelength of at least 30 grid intervals. The asymptotic transfer function itself is computed on the basis of ray theory, for which it is assumed that

$$\frac{1}{v}\frac{dv}{dz} \ll \frac{f}{v}, \tag{28}$$

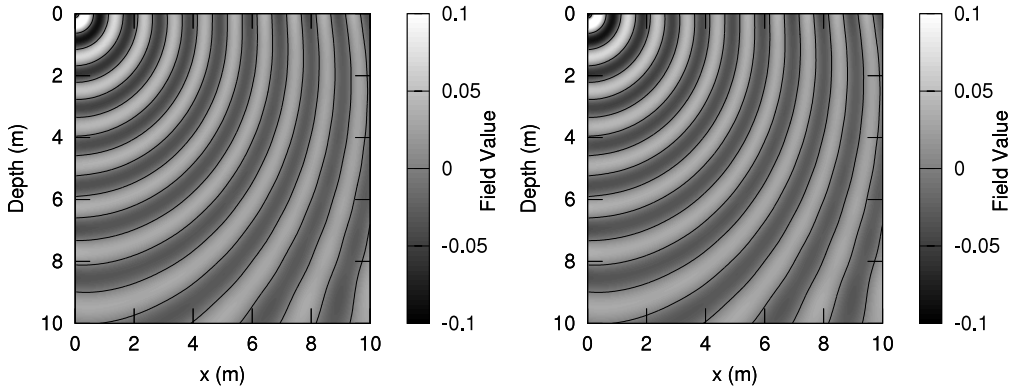

(a) (b)

Figure 5: Two-dimensional wavefield -left panel (a)- obtained by using the full asymptotic transfer function (25) and two-dimensional wavefield -righ panel (b)- obtained by using the far-field approximation of the asymptotic transfer function (27)

where $f = 1$ Hz. The velocity gradient at $z = 10\ m$, corresponding to the deepest ray, *i.e.* $.45\ \ Hz$, which is not much, much less than unity, and thus likely accounts for the discrepancy. A reduction in the velocity gradient will reduce the discrepancy. Indeed, numerical experiments with $b = -0.04\ s^2/m^3$, with $f = 1\ Hz$, demonstrated that this is the case, as shown in Fig. 7. Improvement of the modulus in Figs. 7 and 4 is quite clear as well as for the phase when considering the full asymptotic transfer function. Again, we have an illustration of the importance of the transfer function we should use instead of its far-field approximation which induces in this particular case a phase offset of 0.1° direcly connected to the Hankel function approximation. A secondary phenomenon is also evident in comparing the phases: the oscillation frequency is different between the two

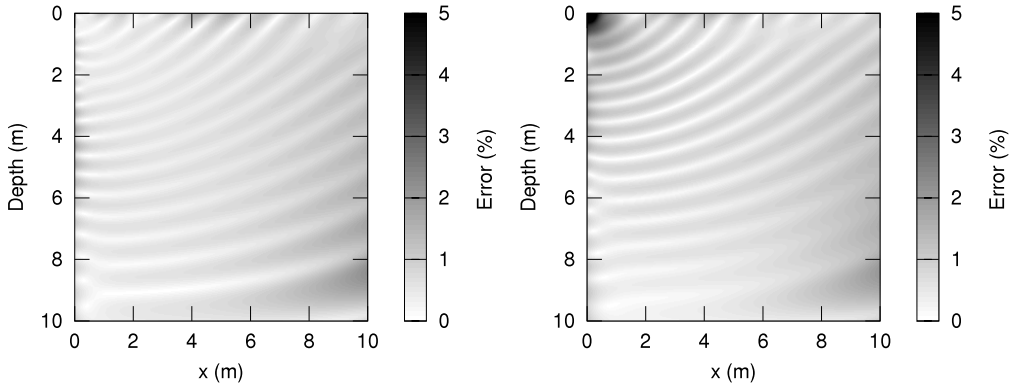

(a) (b)

Figure 6: Error in the reconstructed two-dimensional wavefield -left panel (a)- obtained by using the full asymptotic transfer function (25) and same error -right panel (b)- using the far-field approximation of the asymptotic transfer function (27).

cases. Where do these oscillations come from and why are these oscillations different? The answer is not yet clear and we could infer that it comes from wave interaction with heterogeneities of the medium, corresponding to the two gradients in its particular case. More work is required for a proper quantification of this error.

5. Conclusions

In this paper, we have derived the complete uniform asymptotic expansions that include the source singularity for the Helmholtz equation, in two and three dimensions under the assumption of constant density. From these expansions, we have constructed a transfer function that maps three-dimensional data into two-dimensional data. The transfer function has been

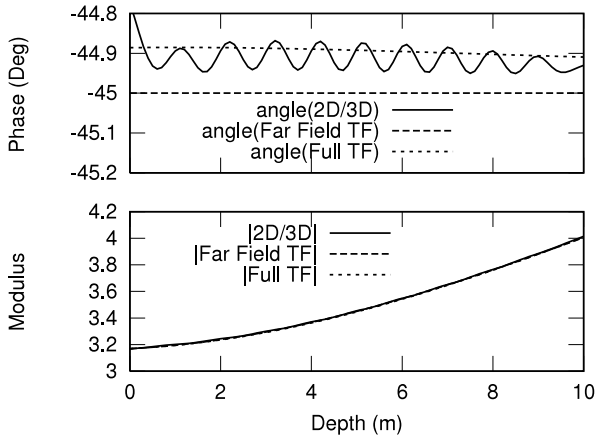

Figure 7: Comparison of phase (upper panel) and modulus (lower panel) of numerical, full and far-field asymptotic transfer functions with $b = -0.04\ s^2/m^3$.

analyzed against numerical solutions of the 2D and 3D Helmholtz equation for a smooth vertically inhomogeneous medium, evaluated for a borehole receiver geometry. We have shown that indeed one should consider the full asymptotic transfer function while its far-field approximation might not be enough especially nearby the source. Future work will extend the foregoing results to more heterogeneous and anelastic media.

Acknowledgments

The authors would like to thank the Canadian and French research agencies for their support. French support was obtained from the ANR under the Project MAXWELL and HPPCO2. Canadian support was obtained from NSERC

References

Avila, G. S. S., Keller, J. B., 1963. The highfrequency asymptotic field of a point source in an inhomogeneous medium. Communications on Pure and Applied mathematics 16 (4), 363–381.

Babich, V., 1965. On the short-wave asymptotic behaviour of the solution of the point source problem in an inhomogeneous medium. Zh.Vychisl.Mat.i Mat.Fiz 5, 949–951.

Babich, V., 1991. On asymptotic solutions of the problems of moving sources of diffusion and oscillations. Journal of Mathematical Sciences 57 (3), 3067–3071.

Bleistein, N., 1986. Twoandonehalf dimensional inplane wave propagation*. Geophysical Prospecting 34 (5), 686–703.

Cerveny, V., 2001. Seismic ray theory. Cambridge Univ Pr.

Chew, W. C., Jin, J. M., Michielssen, E., 1997. Complex coordinate stretching as a generalized absorbing boundary condition. Microwave and Optical Technology Letters 15 (6), 363–369.

Courant, R., Hilbert, D., 1966. Methods of Mathematical Physics. John Wiley, New York.

Ernst, J. R., Green, A. G., Maurer, H., Holliger, K., 2007. Application of a new 2d time-domain full-waveform inversion scheme to crosshole radar data. Geophysics 72, J53.

Karal, F. C., Keller, J. B., 1959. Elastic wave propagation in homogeneous and inhomogeneous media. The Journal of the Acoustical Society of America 31, 694.

Keller, J. B., 1978. Rays, waves and asymptotics1. AMERICAN MATHEMATICAL SOCIETY 84 (5).

Lambaré, G., Lucio, P. S., Hanyga, A., 1996. Two-dimensional multivalued traveltime and amplitude maps by uniform sampling of ray field. Geophys. J. Int. 125, 584–598.

Pratt, R. G., Shin, C., Hicks, G. J., 1998. Gauss-newton and full newton methods in frequencyspace seismic waveform inversion. Geophys.J.Internat 133, 341362.

Pratt, R. G., Song, Z. M., Williamson, P., Warner, M., 1996. Twodimensional velocity models from wideangle seismic data by wavefield inversion. Geophysical Journal International 124 (2), 323–340.

Vidale, D., 1988. Finite-difference calculation of travel time. Bull. seism. Soc .Am. 78, 2062–2076.

Vidale, J., May 1990. Finite-difference calculation of travel times in three dimensions. Geophysics 55 (5), 521–526.

Virieux, J., 1996. Seismic ray tracing. In: Boschi, E., Ekström, G., Morelli, A. (Eds.), Seismic modelling of Earth structure. Editrice Compositori, Bologna, pp. 223–304.

Virieux, J., Lambaré, G., 2007. Theory and observations - body waves: ray methods and finite frequency effects. In: Romanovitz, B., Diewonski, A. (Eds.), Treatise of Geophysics, volume 1: Seismology and structure of the Earth, Treatise of Geophysics. Elsevier.

Williamson, P. R., Pratt, R. G., 1995. A critical review of acoustic wave modeling procedures in 2.5 dimensions. Geophysics 60 (2), 591–595.
URL http://link.aip.org/link/?GPY/60/591/1

Yedlin, M., Virieux, J., 2010. Uniformly asymptotic frequency domain greens functions for the acoustic equation-theory and applications in two and three dimensions. Geophysical Research Abstracts 12, EGU2010-7006-4, 2010.

Yedlin, M. J., 1987. Uniform asymptotic solution for the greens function for the twodimensional acoustic equation. The Journal of the Acoustical Society of America 81, 238.

Zauderer, E., 1970. Uniform asymptotic solutions of the reduced wave equation* 1. Journal of Mathematical Analysis and Applications 30 (1), 157–171.

Zhao, H., 2005. A fast sweeping method for eikonal equations. Mathematics of computation 74 (250), 603–628.